CSIRO PUBLISHING

www.publish.csiro.au/journals/pasa *Publications of the Astronomical Society of Australia*, 2003, **20**, 159–164

Photometry of R Coronae Borealis Stars during the Recovery Phase of their Declines

Lj. Skuljan, P. L. Cottrell, A. C. Gilmore and P. M. Kilmartin

Department of Physics and Astronomy, University of Canterbury, Christchurch, New Zealand
l.skuljan@phys.canterbury.ac.nz
p.cottrell@phys.canterbury.ac.nz
a.gilmore@phys.canterbury.ac.nz
p.kilmartin@phys.canterbury.ac.nz

Received 2002 July 22, accepted 2003 January 14

Abstract: The photometric observations (*UBVRI*) of nine cool R Coronae Borealis (RCB) stars have been collected at Mt John University Observatory, New Zealand, over a period of twelve years. The analysis of the magnitude–colour and colour–colour diagrams for the recovery phase demonstrates that all declines exhibit a similar asymptotic approach to their normal brightness. Declines return to maximum brightness along a line with essentially the same slope that does not depend on the star or the depth of the decline. Assuming a uniform obscuration of the photosphere by the dust cloud during the recovery phase, the extinction properties of the material were determined. The ratio of total to selective extinction (R_V) for the RCB stars in our sample is in the range 2.5 to 4.6, indicating that the obscuring dust has extinction properties similar to that of the interstellar dust. Observations have been compared with the theoretical extinction curves for different sorts of grains.

Keywords: stars: variables: R Coronae Borealis — methods: data analysis

1 Introduction

The R Coronae Borealis (RCB) stars are hydrogen-deficient carbon-rich supergiants, with a characteristic pattern of variability. A significant amount of carbon dust is created in their atmospheres at random intervals, causing the photospheric brightness to drop by up to six magnitudes in a few weeks. Therefore, these stars provide a unique opportunity to study the nature and evolution of the dust material obscuring the photosphere during the decline phase. The environment for studying the carbon grains in RCB stars is quite different from 'normal' carbon stars, which are both carbon-and hydrogen-rich.

A limited number of studies of the extinction properties of the RCB dust can be found in the literature. The UV extinction curves have been obtained for only a few RCB stars (RY Sgr: Clayton et al. 1992; R CrB: Hecht et al. 1984; Holm et al. 1987; V348 Sgr: Jeffery 1995; Drilling et al. 1997; Hecht et al. 1998). In addition, the extinction curves of a few hydrogen-deficient (HdC) stars and other similar objects (such as the Abell 30 nebula) have been compared with the extinction curves of the dust causing the RCB declines (Jeffery 1995). They all show a peak near 2400 Å, which differs from the typical position (2175 Å) obtained from the interstellar medium (ISM).

In this paper the extinction curves in the *UBVRI* region, obtained from the recovery phase photometry of a number of declines of nine RCB stars, will be analysed. The results will then be compared with the extinction curves obtained from the UV spectra of RY Sgr, the ISM and the laboratory data for different particles.

2 Observations

The photometric observations (*UBV* and *UBVRI*) of the nine RCB stars (Table 1) have been obtained at Mt John University Observatory (MJUO) on either the Boller and Chivens or the Optical Craftsmen telescope (both have a diameter of 0.6 m). The telescopes have been equipped with an automated single channel photometer using either an EMI 9558B or 9202B photomultiplier tube. The filters used for the photometric observations are similar to those described by Bessell (1979). The observations were obtained differentially with respect to nearby comparison stars (for more details see Lawson et al. 1990).

The observations extended between 1986 April and 1998 December, which included 26 declines of nine

Table 1. Program stars*

Star	V	$B-V$	$T_{\rm eff}$(K)	$N_{\rm d}$
V854 Cen	7.10	0.50	7000	85
S Aps	9.72	1.21	5000	116
RZ Nor	10.42	1.06	7000	17
UW Cen	9.11	0.67	6800	21
V CrA	9.95	0.72	7000	15
RS Tel	9.94	0.82	7000	51
RY Sgr	6.40	0.62	7000	61
RT Nor	10.14	1.06	7000	14
U Aqr	11.19	0.95	5500	39

* Maximum visual magnitude (V), colour ($B-V$) and $T_{\rm eff}$ are taken from Lawson et al. (1990); $N_{\rm d}$ is the number of data points used for analysis.

10.1071/AS02024 1323-3580/03/02159

different RCB stars. The stars have been observed at maximum light as well as during the declines. The main emphasis in this paper is on analysing photometry during the recovery from a deep decline, although changes in the magnitude–colour diagrams throughout the whole decline are also noted. The nine RCB stars studied in this paper are listed in Table 1 with some of their basic parameters.

The mean V magnitude and colours for each star are normally obtained by averaging over several ($\sim$3−6) successive measurements. When the star is brighter than $V \approx 11^{\rm m}$, a typical precision in V is about $0\overset{\rm m}{.}02$, while it is slightly worse for the colours ($0\overset{\rm m}{.}03$ for $B-V$, $V-R$ and $V-I$, and $0\overset{\rm m}{.}04$ for $U-B$). During a decline, when the star is significantly fainter, a typical uncertainty in V is less than about $0\overset{\rm m}{.}03$, while it can be as high as $0\overset{\rm m}{.}04$ for $B-V$, $V-R$ and $V-I$, and $0\overset{\rm m}{.}05$ for $U-B$. In this analysis we have formed the colour $U-V$ to calculate the normalised extinction in U with respect to V (see Section 3, Table 2).

3 Recovery Phase Photometry

Both the photometric magnitudes and colours show significant changes during an RCB decline (Figure 1). The light curve asymmetry, generally with a rapid decline and a slow recovery, is accompanied by unusual colour behaviour.

Table 2. The line slopes from the magnitude–colour and colour–colour diagrams

Star	R_V	$\frac{\Delta V}{\Delta(U-V)}$	$\frac{\Delta V}{\Delta(V-R)}$	$\frac{\Delta V}{\Delta(V-I)}$	$\frac{\Delta(U-V)}{\Delta(B-V)}$	$\frac{\Delta(V-R)}{\Delta(B-V)}$	$\frac{\Delta(V-I)}{\Delta(B-V)}$
S Aps	4.0 ± 0.2	1.4 ± 0.2	7.4 ± 0.3	3.7 ± 0.2	2.3 ± 0.1	0.5 ± 0.1	1.0 ± 0.1
U Aqr	3.3 ± 0.4	1.3 ± 0.3			2.1 ± 0.1		
UW Cen	3.0 ± 0.3	1.3 ± 0.2	5.7 ± 0.2		2.2 ± 0.1	0.3 ± 0.1	
V854 Cen	3.6 ± 0.2	1.6 ± 0.2	5.9 ± 0.3	3.2 ± 0.2	1.9 ± 0.1	0.57 ± 0.10	1.1 ± 0.10
RZ Nor	3.4 ± 0.3	1.5 ± 0.2			2.0 ± 0.1		
RT Nor	3.4 ± 0.4	1.3 ± 0.3			2.4 ± 0.3		
RS Tel	4.6 ± 0.2	1.8 ± 0.2			2.4 ± 0.1		
V CrA	3.7 ± 0.3	1.5 ± 0.2			2.4 ± 0.1		
RY Sgr	2.6 ± 0.3	1.0 ± 0.2	5.4 ± 0.5	2.8 ± 0.2	2.4 ± 0.1	0.5 ± 0.10	0.9 ± 0.1
All stars	3.4 ± 0.1	1.3 ± 0.1	6.2 ± 0.2	3.1 ± 0.1	2.17 ± 0.04	0.48 ± 0.05	1.0 ± 0.05

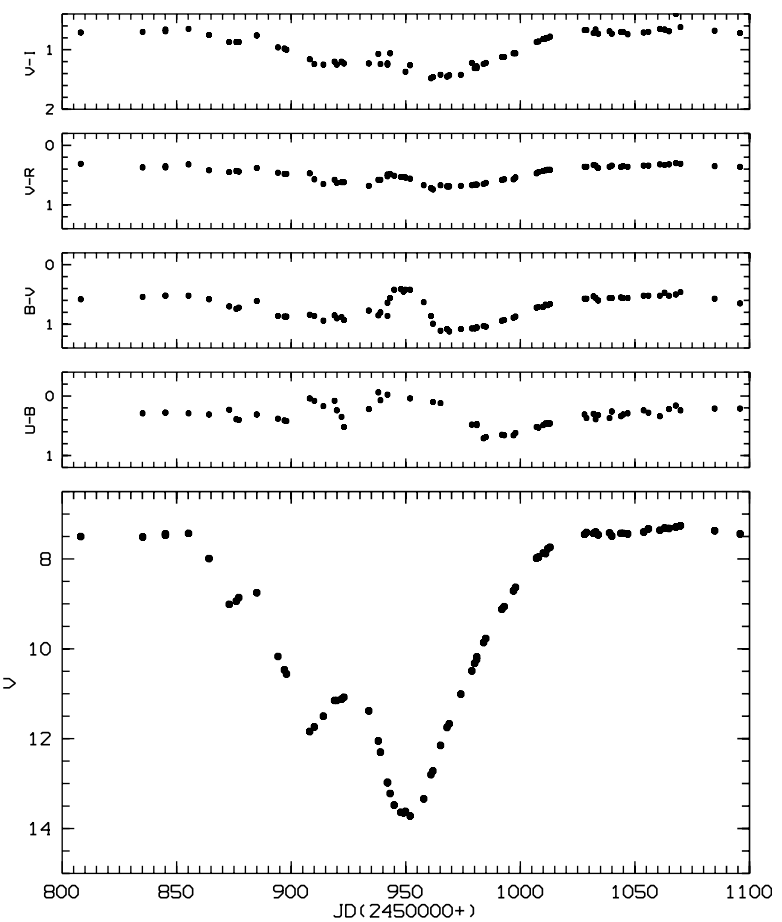

Figure 1 Visual magnitude and colour changes during a typical RCB decline (1998 decline of V854 Cen).

https://doi.org/10.1071/AS02024 Published online by Cambridge University Press

A noticeable colour excess in $B-V$, $U-B$, $V-R$ and $V-I$ is always observed during the recovery phase. However, significantly smaller colour changes are usually found during the initial decline stage, when the brightness is dropping rapidly. This characteristic photometric behaviour can be explained by the appearance and expansion of a dust cloud above the surface of the star (Pugach 1991). During the initial decline phase a newly formed dust cloud is only partially covering the photosphere, while during the recovery stage one can assume that the dust is uniformly distributed over the entire stellar disc.

The magnitude–colour diagrams show a characteristic 'loop' throughout the entire decline phase (Figure 2). As the star approaches its maximum brightness (during the late recovery stage) the data points tend to follow an asymptote, as indicated by a straight line in each of the panels in Figure 2. The asymptotic approach to the normal brightness has been observed in all RCB declines. Moreover, the slope of the asymptotic line is independent of the depth of the decline and is almost the same value for all RCB stars. The asymptote represents a common line along which the colour indices would vary if the star brightness faded due to total obscuration of the photosphere by a uniform dust cloud.

The slope in the magnitude–colour and colour–colour diagrams (see Figure 3) for the recovery decline phase can be used in determining the optical properties of the dust causing the decline. When these diagrams are constructed relative to the light maximum, any permanent contribution (such as circumstellar and interstellar dust) to the extinction cancels out and so only the contribution from the newest dust cloud will remain.

In determining the optical properties of the dust around the RCB stars one has to assume that the dust distribution is uniform over the entire stellar disc. Any partial coverage of the photosphere by a localised dust cloud (which is the case during the initial stages of the decline) will result in an overestimation of the slope in the magnitude–colour planes. One can assume that the conditions of a uniform distribution are fulfilled during the recovery phase (from a few magnitudes below the maximum), when the dust cloud covers the entire photosphere. The magnitude threshold used in this analysis has been chosen depending on the actual depth of the decline. It is generally between one and two magnitudes below the light maximum, when the data points roughly follow a straight line in the magnitude–colour diagram. All data points that fall below this threshold were rejected.

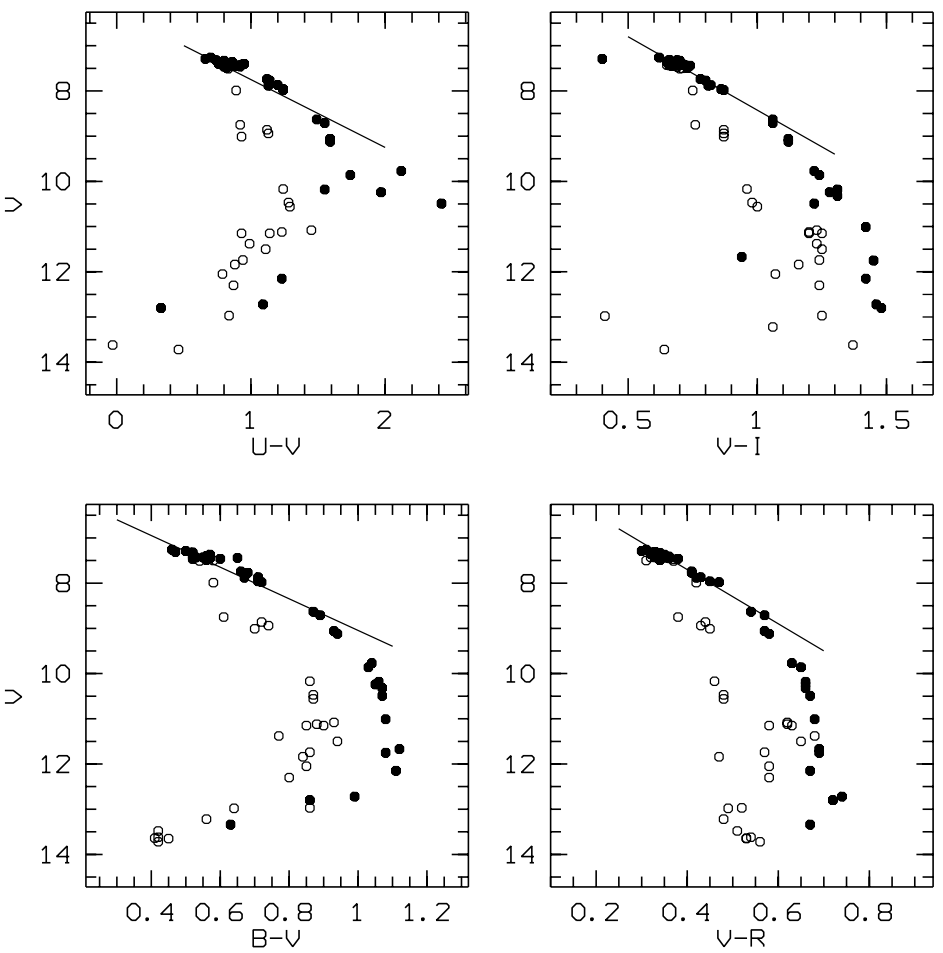

Figure 2 The magnitude–colour diagrams for the 1998 decline of V854 Cen. Open circles represent the initial decline phase, while filled dots are used for the recovery phase.

https://doi.org/10.1071/AS02024 Published online by Cambridge University Press

The magnitude–colour and colour–colour diagrams have been examined for all declines of each star separately, as well as for all RCB declines together (Table 2). In the latter case, the average magnitude and colours at maximum light have been subtracted from the photometric data for each star, so that all measurements have the same zero point. These diagrams are shown in Figure 3 with the line slopes listed in the last row of Table 2. The uncertainties in the slopes are not only affected by the measurement uncertainties in the photometry, but also by the amplitude

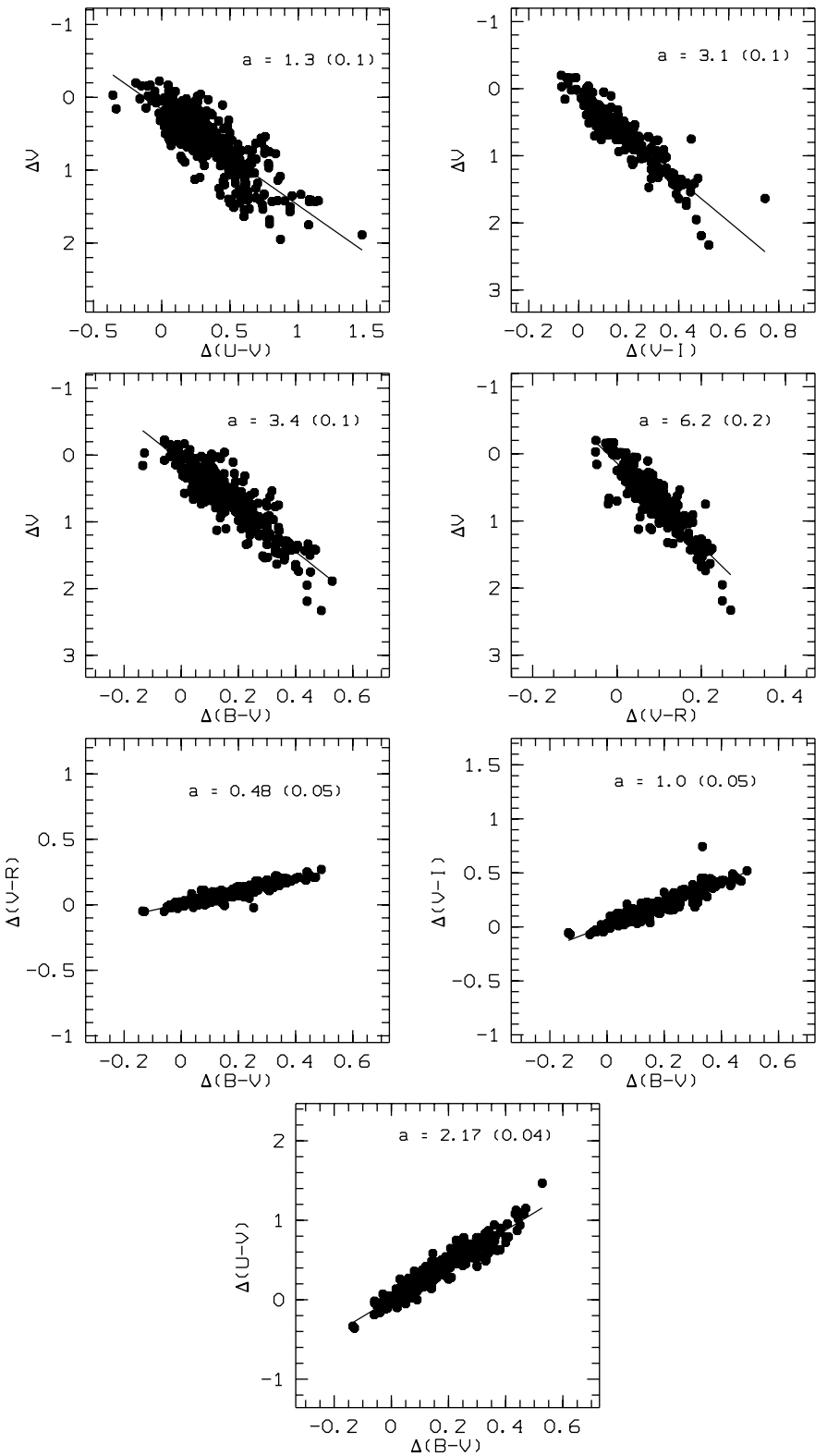

Figure 3 The adjusted zero point (see text) magnitude–colour and colour–colour diagrams for the recovery data for all RCB stars from this study. The slopes of the linear fit (a), with σ in brackets, are also given.

https://doi.org/10.1071/AS02024 Published online by Cambridge University Press

variations (pulsations) both in stellar magnitudes and colours, especially in RY Sgr ($\Delta V \sim 0\overset{m}{.}6$).

The normalised extinction of the RCB dust, A_λ/A_V, has been calculated from the equation

$$\frac{A_\lambda}{A_V} = 1 + \frac{E(m_\lambda - V)}{A_V}, \qquad (1)$$

where A_V (the total extinction in V) can be expressed in terms of the ratio of total to selective extinction

$$R_V = \frac{A_V}{E(B\text{–}V)}. \qquad (2)$$

One can use this relation to obtain the visual absorption A_V from the colour excess $E(B\text{–}V) = (B\text{–}V) - (B\text{–}V)_\circ$ alone. Using equations (1) and (2), A_λ/A_V can be expressed as

$$\frac{A_\lambda}{A_V} = 1 + \frac{1}{R_V}\frac{E(m_\lambda - V)}{E(B\text{–}V)} = 1 + \frac{X_\lambda}{R_V}, \qquad (3)$$

where the colour excess $E(m_\lambda - V)$ now appears normalised with respect to $E(B\text{–}V)$. The ratio, $X_\lambda = E(m_\lambda - V)/E(B\text{–}V)$, can be obtained as the slope in the colour–colour diagrams, $\Delta(m_\lambda - V)/\Delta(B\text{–}V)$, during the recovery phase. On the other hand, the ratio of total to selective extinction, R_V, can be obtained from the $(B\text{–}V, V)$ diagram, as the slope $\Delta V/\Delta(B\text{–}V)$.

4 Discussion

The values of A_λ/A_V have been calculated from equation (3) and then plotted versus λ^{-1}, together with the interstellar (IS) extinction and various observational and laboratory data (Figure 4). The IS extinction was obtained from the analytical relation $A_\lambda/A_V = a(x) + b(x)/R_V$ (Cardelli, Clayton, & Mathis 1989). The curve represents the mean IS extinction law for $R_V = 3.1$, which matches the observational data obtained by Seaton (1979) for $1/\lambda < 7\,\mu\text{m}^{-1}$.

Observations for RY Sgr (taken from Hecht et al. 1984) are also shown in Figure 4, as an example of the UV extinction data for RCB stars. The data exhibit a strong extinction peak near $\lambda = 2400$ Å ($1/\lambda = 4.1\,\mu\text{m}^{-1}$), which differs from $\lambda = 2175$ Å ($1/\lambda \approx 4.6\,\mu\text{m}^{-1}$) in the ISM. A similar extinction peak in the UV region has been obtained from the mean extinction curve of five HdC stars (Jeffery 1995). This is also shown in Figure 4. The HdC extinction curve represents a Gaussian fit (FWHM $= 1.79\,\mu\text{m}^{-1}$, $1/\lambda_{\text{cen}} = 4.07\,\mu\text{m}^{-1}$) through observations of two cool RCB stars (RY Sgr and R CrB, $T_{\text{eff}} \sim 7000$ K) and two hot ones (V348 Sgr and MV Sgr, $T_{\text{eff}} \sim 20000$ K). The data also include a high-excitation planetary nebula (Abell 30), in which the hot central star seems to have ejected a number of hydrogen-poor dust clouds.

The best agreement between the observed extinction curves for the RCB stars and the theoretical models of different dust grains can be obtained for amorphous carbon. The laboratory data for amorphous carbon grains of two different sizes, 30 nm and 8 nm (Borghesi, Bussoletti, & Colangeli 1985), are shown in Figure 4. The UV extinction peak of the amorphous carbon coincides with the RCB data in the same region. The curves also agree with the *UBVRI* extinction obtained from the recovery phases of the sample of nine RCB stars. The normalised absorption for the observed RCB stars in the U region differs slightly from the mean IS curve. This value is similar to the mean UV extinction curve for the HdC stars, and the laboratory data for amorphous carbon grains of 8 nm. The difference between the RCB data in the U region and 30 nm laboratory data is small and possibly not significant taking into account the uncertainties.

Hecht et al. (1984) have compared the observational data for RY Sgr and R CrB with calculated theoretical

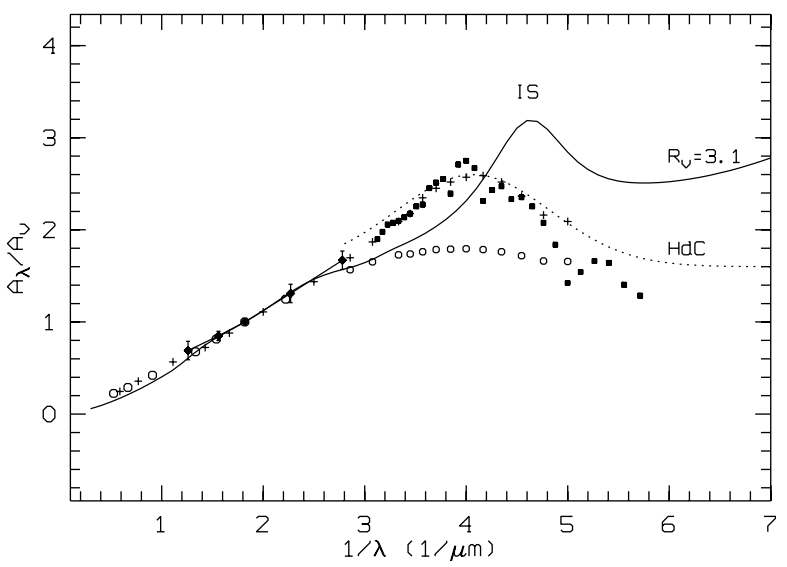

Figure 4 The observed extinction for the nine RCB stars (filled diamonds) with error bars, compared with the IS extinction curve (bold line), HdC extinction (dashed line), UV data for RY Sgr (filled squares), and laboratory data for amorphous carbon particles of 8 nm (crosses) and 30 nm (open circles).

https://doi.org/10.1071/AS02024 Published online by Cambridge University Press

extinction curves for the amorphous and graphite particles of different size. The amorphous carbon spheres between 15 and 50 nm give the best fit for RY Sgr, while the extinction curve for R CrB fits the smaller (10–35 nm) either graphite or amorphous carbon particles. The same authors also indicate that the ratio of total to selective extinction (R_V) changes with the particle size throughout the decline. The larger values for R_V (>4), appearing during the deep minimum, correspond to the bigger particles that are gradually replaced by smaller particles ($R_V < 4$) during the later part of the recovery phase. Hecht et al. (1984) found R_V of 2.8 and 3.14 for RY Sgr and R CrB respectively, similar to the values for our sample of RCB stars (between 2.6 and 4.6). Similar R_V (~ 3) have also been observed for R CrB (Fernie, Sherwood, & DuPuy et al. 1972; Pugach & Kovalchuck 1988).

The difference in the positions of the UV peaks in the RCB dust and IS extinction curves can be explained by the different nature of the dust particles responsible for the extinction in these two cases. The UV peak in the IS extinction curve is mainly caused by graphite particles, which can only form in the presence of hydrogen. On the other hand, the amorphous carbon can form in the hydrogen-poor atmospheres of RCB stars (Hecht et al. 1984; Hecht 1991). Comparing the extinction curves of the RCB dust with the ISM, one can also notice that the overall extinction in the far UV is considerably lower in the RCB dust than in the ISM. This lower extinction is closer to the behaviour of the dense ISM with higher values ($R_V > 3.1$) of the ratio of total to selective extinction.

5 Conclusion

The photometric observations (*UBVRI*) of nine cool RCB stars have been collected at MJUO over a period of twelve years. Analysis of the recovery phase magnitude–colour diagrams of 26 different declines of these stars has been made in order to determine the extinction properties of the dust.

The photometric magnitudes and colours show significant changes during the RCB declines. The asymptotic approach to normal brightness can be seen in the magnitude–colour diagrams of the recovery phase. This is observed for all RCB declines and, without exception, is independent of their decline amplitude. According to the most acceptable theory, the distribution of the dust matter in the cloud which causes the light fading can be considered uniform as the stars recover to their maximum brightness. Then the slopes of the magnitude–colour and colour–colour diagrams from this phase can be used in defining the normalised extinction quantity A_λ / A_V.

Although the extinction curve in the *UBVRI* region is not a good indicator of the type and size of the particles, our data show that the material causing the RCB declines has extinction properties similar to that of the interstellar medium. The ratio of total to selective extinction (R_V) for the RCB stars in our sample is in the range 2.5 to 4.6, similar to that for the interstellar dust. In order to obtain more precise characteristics of the RCB dust one has to examine the extinction data in the UV region, where the extinction curves are more sensitive to the nature of the material.

Acknowledgments

LS would like to acknowledge financial support from a University of Canterbury Doctoral Scholarship, a Marsden Fund studentship and an Amelia Earhart Award. PLC would like to acknowledge support from a Marsden Fund grant entitled ‘Stellar Astrophysics’.

References

Bessell, M. S. 1979, PASP, 91, 589
Borghesi, A., Bussoletti, E., & Colangeli, L. 1985, A&A, 142, 225
Cardelli, J. A., Clayton, G. C., & Mathis, J. S. 1989, ApJ, 345, 245
Clayton, G. C., Whitney, B. A., Stanford, S. A., & Drilling, J. S. 1992, ApJ, 397, 652
Drilling, J. S., Hecht, J. H., Clayton, G. C., Mattei, J. A., Landolt, A. U., & Whitney, B. A. 1997, ApJ, 476, 865
Fernie, J. D., Sherwood, V., & DuPuy, D. L. 1972, ApJ, 172, 383
Hecht, J. H. 1991, ApJ, 367, 635
Hecht, J. H., Holm, A. V., Donn, B., & Wu, C.-C. 1984, ApJ, 280, 228
Hecht, J. H., Clayton, G. C., Drilling, J. S., & Jeffery, C. S. 1998, ApJ, 501, 813
Holm, A. V., Hecht, J., Wu, C.-C., & Donn, B. 1987, PASP, 99, 497
Jeffery, C. S. 1995, A&A, 299, 135
Lawson, W. A., Cottrell, P. L., Kilmartin, P. M., & Gilmore, A. C. 1990, MNRAS, 247, 91
Pugach, A. F. 1991, SvA, 35, 61 (AZh, 68, 122, in Russian)
Pugach, A. F., & Kovalchuck, G. U. 1988, IBVS, 3147
Seaton, M. J. 1979, MNRAS, 187, 73P